Disorder-Induced Capillary Bursts Control Intermittency in Slow Imbibition

Xavier Clotet,[1,2] Jordi Ortín,[1] and Stéphane Santucci[2]
[1]Departament ECM, Facultat de Física, Universitat de Barcelona, Martí i Franquès 1, 08028 Barcelona, Catalonia, Spain
[2]Laboratoire de Physique, CNRS UMR 5672, École Normale Supérieure de Lyon, 46 Allée d'Italie, 69364 Lyon Cedex 07, France
(Received 11 October 2013; published 13 August 2014)

A multiscale analysis of the spatially averaged velocity of an imbibition front $V_\ell(t)$ measured at scale ℓ reveals that the slow front dynamics is intermittent: the distributions of $\Delta V_\ell(\tau) = V_\ell(t+\tau) - V_\ell(t)$ evolve continuously through time scales τ, from heavy-tailed to Gaussian—reached at a time lag τ_c set by the extent of the medium heterogeneities. Intermittency results from capillary bursts triggered from the smallest scale of the disorder up to the scale ℓ_c at which viscous dissipation becomes dominant. The effective number of degrees of freedom of the front ℓ/ℓ_c controls its intensity.

DOI: 10.1103/PhysRevLett.113.074501 PACS numbers: 47.56.+r, 05.40.-a, 47.53.+n

The heterogeneous structure of porous and fractured media can lead to complex spatiotemporal fluid invasion dynamics, with kinetic roughening [1–4], avalanches [5–8], and non-Gaussian velocity fluctuations [5–7,9] of the invading fronts. It, thus, brings forward challenging fundamental questions in the context of out-of-equilibrium dynamical systems [10], relevant to many processes of interest [11].

Among the striking spatiotemporal features of porous media flows, persistent intermittent properties of Lagrangian velocities have been observed very recently in numerical simulations [12]. Intermittency is a key concept in hydrodynamic turbulence, associated with the occurrence of bursts of intense motion within more quiescent fluid flow [13]. It leads to strong deviations from Gaussian statistics, that become larger when considering fluctuations at smaller scales [14,15]. In the context of interfacial dynamics, small-scale intermittency was observed in gravity-capillary wave turbulence [16], a system which strongly differs from high Reynolds hydrodynamic turbulence [17]. Thus, understanding the physical mechanism of intermittency remains a challenge [16–20]. Recently, it was suggested that it could be related to the properties of the fluctuations of the energy flux shared by different systems displaying an energy cascade [16,17].

In this Letter, we perform a multiscale analysis (in space and time) of the spatially averaged velocity of a fluid front slowly invading a disordered medium. While in Ref. [6] we studied the statistical properties of this velocity, the novel study presented here reveals that this velocity displays complex temporal correlations and exhibits all the distinguishing features of an intermittent dynamics. More importantly, expanding the experimental parameter space by using fluids of different viscosities and a wider range of imposed flow rates, we disclose which variables control intermittency in this system. Our work provides the first experimental evidence and detailed characterization of intermittency in fluid invasion of confined heterogeneous media, and brings new insight into the origin of intermittency in extended nonequilibrium systems.

Our experiments emulated the invasion of an open fracture of variable aperture by a wetting, viscous fluid. The experimental setup, shown in the top panel of Fig. 1, has been described in detail elsewhere [4,7]. We recall, briefly, its main features. It consists of two horizontal, parallel glass plates (190×500 mm^2), separated by a narrow gap spacing. Nonoverlapping square patches (0.4×0.4 mm^2) randomly distributed in space and filling 35% of the bottom plate provide dichotomic fluctuations of the gap thickness between 0.40 and 0.46 mm, modifying the permeability κ of the cell [21]. In these conditions, the lateral extent of the islands formed by adjacent patches

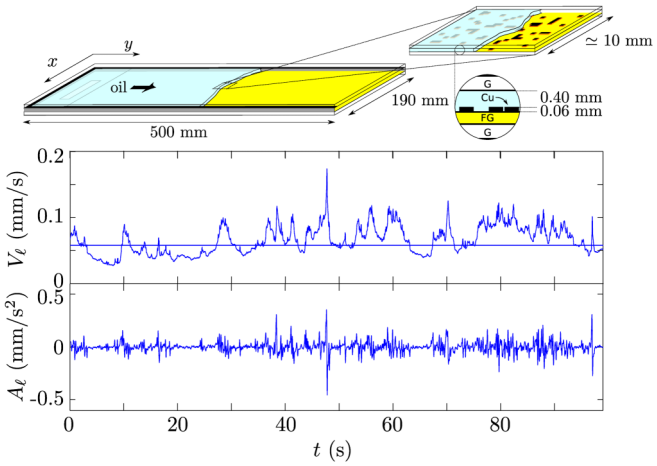

FIG. 1 (color online). Top: Sketch of the model disordered medium. It is formed by two parallel, closely spaced glass plates (G). Copper patches (Cu) of lateral size 0.4×0.4 mm^2 and 0.06 mm height, randomly deposited without overlapping, cover 35% of the bottom fiber glass plate (FG). Middle: Global velocity, $V_\ell(t)$, computed from an experiment with v = 0.053 mm/s and $\mu = 50$ cP ($\ell_c \simeq 11$ mm), observed on a scale $\ell = L/8 = 17$ mm. Bottom: Corresponding time-derivative, $A_\ell(t)$.

follows an exponential distribution, with a characteristic length $\ell_d = 0.6$ mm [8]. Silicone oil was injected at a constant flow rate, and displaced the air initially present. The nearly flat initial front became progressively rougher, until a statistically stationary state was reached in which the front width saturated to a constant value. We recorded the advancement of the fluid front, in the stationary state, with high spatial and temporal resolution ($r = 0.106$ mm/pixel and up to 200 frames/s). The size of the recorded frames was $L = 136$ mm in the transverse direction (x) and 25 to 45 mm in the propagation direction (y).

We used silicone oils of five different dynamic viscosities, from $\mu = 10$ to 350 cP, and similar oil-air surface tension around $\gamma = 21$ mN/m. The imposed flow rates produced mean front velocities in the range $0.04 < \mathrm{v} < 0.6$ mm/s, giving capillary numbers $\mathrm{Ca} = \mu \mathrm{v}/\gamma$ between 6×10^{-5} and 2×10^{-3}. For each given experimental condition (v, μ), we performed 15 to 20 experiments with different disorder realizations. The interface profiles $h(x,t)$ were obtained from the recorded snapshots by applying an edge-tracking algorithm. Measuring the amount of time spent by the front on each (x,y) position, $wt(x, y = h(x,t))$, we computed the map of local front velocities $v(x,y) = r/wt(x,y)$ [22], where r is the spatial resolution specified earlier. Finally, the global velocity of the front on scale ℓ was obtained by averaging a spatiotemporal map $v(x,t)$ of these local velocities over a window of lateral size ℓ, $V_\ell(t) = (1/\ell)\int_\ell v(x,t)dx$. Figure 1 shows a typical velocity signal $V_\ell(t)$, and its time derivative.

Because of the medium heterogeneities, capillary pressure and permeability variations distort the imbibition front, while viscous pressure and surface tension tend to restore its flatness (see the videos in the Supplemental Material [23]). For slow displacements (capillary regime) the oil-air interface develops long range correlations, with a lateral correlation length given by the crossover length scale $\ell_c = \sqrt{\kappa/\mathrm{Ca}}$ at which viscosity becomes more effective than surface tension in damping the capillary-pressure fluctuations [3,7,10]. For fast displacements, both capillary-pressure and permeability fluctuations become relevant [7]. In contrast to the dynamics observed in a compact porous medium with characteristic pore size bursts [24], the interfacial dynamics in our disordered confined medium consists of power-law distributed avalanches, both in sizes and durations. Their cutoffs imposed by the finite correlation length ℓ_c diverge for $\mathrm{v} \to 0$ [8], signaling the presence of a critical depinning transition [10]. Within the range of parameters explored in the present experiments, corresponding to slow displacements, the lateral correlation length took values in the range $3 < \ell_c < 15$ mm, much larger than the spatial resolution of the images and the characteristic length of the medium heterogeneities, $\ell_d = 0.6$ mm. The possibility of tuning independently ℓ_c and ℓ allowed experimental studies of "finite-size scaling," a tool often used in theoretical analysis of critical phenomena [25].

Spatially localized avalanches, which may occur simultaneously along the interface, can lead to strong temporal fluctuations of the global advancement of the imbibition front. In order to study the fluctuations of the spatially averaged (global) velocity $V_\ell(t)$, and specifically its intermittent character, we performed a multiscale analysis of the signal with the multifractal formalism introduced by Parisi and Frisch for fully developed turbulence [13]. We examined the statistical properties of the velocity increments $\Delta V_\ell(\tau) = V_\ell(t+\tau) - V_\ell(t)$ for various time delays τ and length scales ℓ. First, we present the results corresponding to a given set of conditions: $\mathrm{v} = 0.053$ mm/s and $\mu = 50$ cP, with a measuring window $\ell = L/8 = 17$ mm ($\simeq 1.6\ell_c$). Figure 2 (top panel) shows the distributions of the normalized velocity increments $Y = (\Delta V_\ell - \langle \Delta V_\ell \rangle)/\sigma$ for increasing time lags τ. $\langle \Delta V_\ell \rangle$ stands for the ensemble average of ΔV_ℓ and σ for its standard deviation. Interestingly, we observe that the shape of these distributions evolved through the temporal scales τ. For short time lags, we measured distributions with exponential tails and a peak at $Y = 0$ (zero acceleration). This shape progressively evolved towards nearly Gaussian

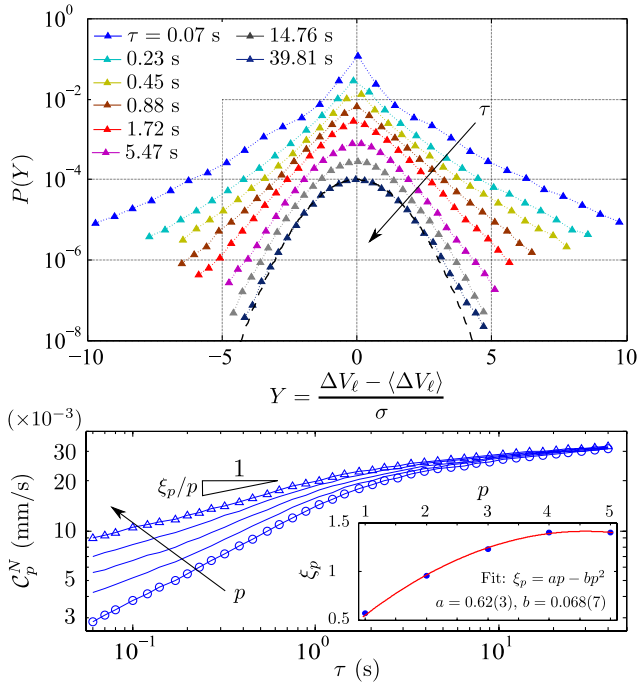

FIG. 2 (color online). Top: semilog plot of $P(Y)$ vs $Y = (\Delta V_\ell - \langle \Delta V_\ell \rangle)/\sigma$ for increasing time lags τ, shifted vertically for visual clarity, for experiments at $\mathrm{v} = 0.053$ mm/s and $\mu = 50$ cP, and analyzed at $\ell = L/8 = 17$ mm. The dashed curve represents a Gaussian pdf. Bottom: Corresponding p-root normalized structure functions $C_p^N(\tau)$ for $p = \{1(\circ), 2, 3, 4, 5(\triangle)\}$. The inset shows the evolution of the exponent ξ_p with p; error bars are smaller than symbol size.

distributions at longer time lags. This result unveils that the dynamics of the invading front is highly intermittent, with complex temporal correlations on short time intervals, which we quantified through the analysis of the fluctuations of $V_\ell(t)$. The fluctuations are locally described by the singularity exponents $h(t)$ given by $\Delta V_\ell(\tau) \sim \tau^{h(t)}$ as $\tau \to 0^+$. Nonlocal singularities can be characterized by the p-order structure functions $\mathcal{S}_p(\tau) \equiv \langle |\Delta V_\ell(\tau)|^p \rangle$, from which the spectra of global exponents ξ_p can be defined as $\mathcal{S}_p(\tau) \sim \tau^{\xi_p}$. Homogeneous fluctuations [$h(t) = H$ for all t] lead to $\xi_p \sim p$, while nonhomogeneous temporal fluctuations whose singularity exponents vary with time—a hallmark of intermittency—result in a nonlinear dependence of ξ_p with p [26,27]. In order to unveil deviations from monofractality and Gaussian statistics, we computed the normalized p-root structure functions $\mathcal{C}_p^N(\tau) \equiv \mathcal{C}_p/\mathcal{R}_p^G$, where $\mathcal{C}_p \equiv \mathcal{S}_p^{1/p}$ and the normalizing factor $\mathcal{R}_p^G \equiv (\mathcal{S}_p^G/\mathcal{S}_2^G)^{1/p}$ is the ratio of structure functions for a Gaussian distribution, which depends only on p [28]. The bottom panel of Fig. 2 shows a double-logarithmic plot of $\mathcal{C}_p^N(\tau)$ for $p = 1, \ldots, 5$. At short time lags, $\mathcal{C}_p^N \sim \tau^{\xi_p/p}$ over more than one decade. The inset shows that ξ_p depends nonlinearly on p, reflecting the intermittent dynamics of $V_\ell(t)$. At large τ, $\mathcal{C}_p^N(\tau)$ collapsed onto a single curve for all p as expected for Gaussian statistics – observed in the top panel of Fig. 2.

Intermittency was observed for all the experimental conditions explored. But, more interestingly, we noticed that the tails of the distributions of velocity increments for a given time lag τ were systematically larger in some limits—thus, revealing a stronger intermittent character. Larger tails were observed when either $V_\ell(t)$ was measured at smaller length scales ℓ [29] or the imposed flow rate (and hence, v) or the oil viscosity μ were smaller, as shown in Fig. 3. To quantify this systematic evolution, we computed the kurtosis K (a measurement of the relative importance of the tails) and skewness Sk (a measurement of the asymmetry) of the ΔV_ℓ distributions [30]. The bottom panel of Fig. 4 shows the systematic decrease of K for various ℓ towards a plateau at large time lags, for a given set of experiments performed at v = 0.13 mm/s and $\mu = 50$ cP. For measuring windows larger than the lateral extent of correlated motion $\ell > \ell_c$, K reached the expected Gaussian value $K_G = 3$, but it was significantly larger for $\ell < \ell_c$ due to finite-size effects. The decrease of the kurtosis at short τ could be approximated by a power law $K \sim \tau^{-\alpha}$, reflecting the nonsimilarity of the statistical distributions at different time lags, and thus, once again, intermittent temporal fluctuations of the global front velocity up to a characteristic time τ_c, as observed previously in Fig. 2. The exponent α measuring the intensity of the intermittent character of the velocity signal [20] increased systematically as ℓ approached ℓ_c and saturated to a nearly constant value for $\ell \leq \ell_c$, as shown in the inset of Fig. 4. It is worth noting that, in addition to being heavy tailed, the distributions for short τ had a small positive asymmetry, which decreased systematically with ℓ, as shown in the top panel of Fig. 4.

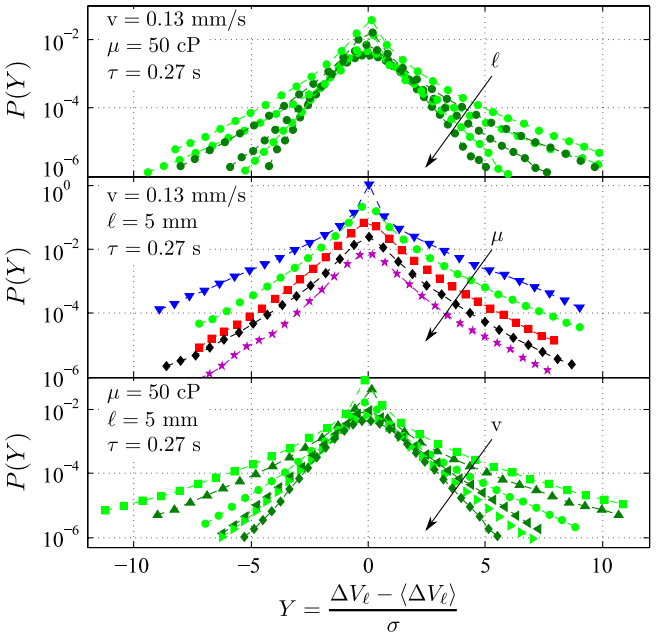

FIG. 3 (color online). Evolution of the normalized distributions of velocity increments with the window of observation ℓ (top), viscosity μ (middle), and imposed mean velocity v (bottom). Range of parameters explored: $\ell = 136$, 34, 12.4, 6.5, 4.3, 2.7 mm; $\mu = 10$, 50, 100, 169, 350 cP; and v = 0.036, 0.053, 0.13, 0.23, 0.35, 0.55 mm/s. Distributions are shifted arbitrarily for visual clarity.

To compare the various experiments performed in very different conditions, and avoid finite-size effects due to the correlation length scale ℓ_c (and specifically, its evolution with v and μ), we carried out the same analysis for spatially averaged velocity V_ℓ measured at scales ℓ such that ℓ/ℓ_c

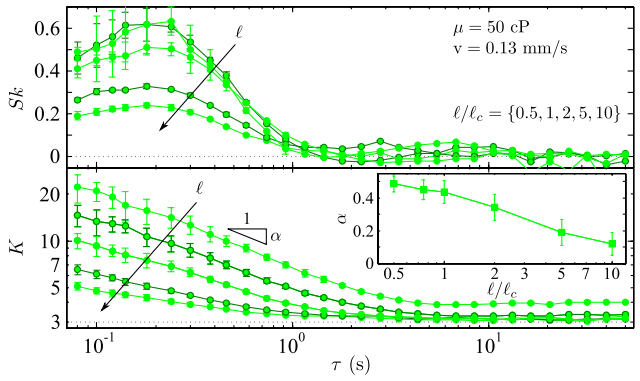

FIG. 4 (color online). Semilog plot of the skewness (top) and log-log plot of the kurtosis (bottom) of $P(\Delta V_\ell)$ for various ℓ as function of τ. The horizontal dashed line corresponds to $K_G = 3$. The inset shows the exponent α of the power-law decay of the kurtosis as a function of ℓ/ℓ_c. In these experimental conditions $\ell_c = 6.7$ mm.

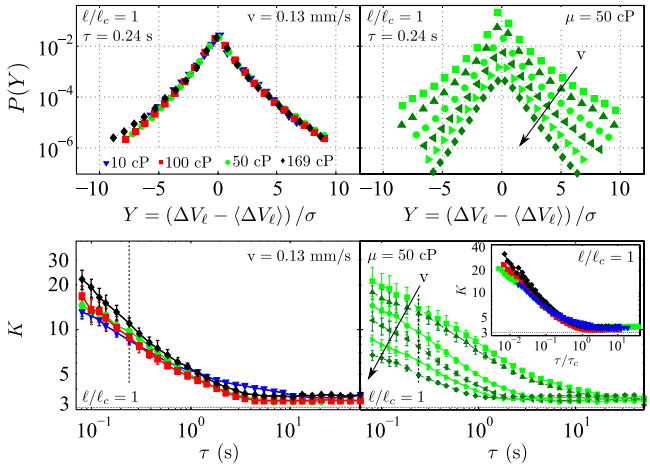

FIG. 5 (color online). Semilog plots of the normalized distributions of velocity increments (shifted arbitrarily for different v for visual clarity) for experiments analyzed at $\ell = \ell_c$ (top) and log-log plots of their corresponding kurtosis for all time lags τ explored (bottom). Left panels display results for different μ but fixed v. Right panels display the systematic evolution with v (from 0.036 to 0.55 mm/s) for a single μ. Vertical lines give the value of τ used to compute the distributions shown in the top panels. Inset: collapse of the kurtosis for all experiments analyzed at $\ell = \ell_c$ when τ is rescaled by $\tau_c = \ell_d/\mathrm{v}$.

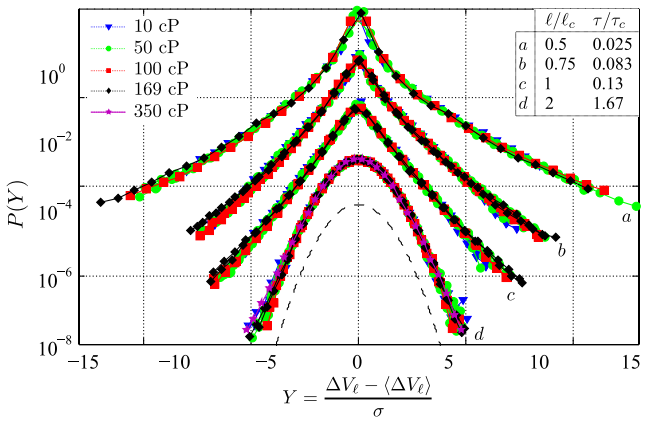

FIG. 6 (color online). Distributions of $\Delta V_\ell(\tau)$ for very different experimental conditions, with v ranging from 0.036 to 0.55 and μ from 10 to 350 cP, collapsed for fixed $(\ell/\ell_c, \tau/\tau_c)$. The dashed curve represents a Gaussian pdf. Distributions are shifted arbitrarily for visual clarity.

was constant. This ratio provides an estimate of the effective number of statistically independent degrees of freedom of the invading front, which controls the non-Gaussian asymmetric shape of the distributions of velocity fluctuations [6]. Interestingly, when measured at scales $\ell = \ell_c$ and a given time lag τ, we observed that the distributions of velocity increments $\Delta V_\ell(\tau)$ collapsed into the same shape for experiments performed at different viscosities but the same velocity (left top panel in Fig. 5). However, in these conditions the shape of the distributions of the velocity increments still evolved systematically with the imposed flow rate (right top panel in Fig. 5). Such behavior is confirmed by the temporal evolution of the kurtosis K for V_ℓ measured at scales $\ell = \ell_c$, as shown in the bottom panels of Fig. 5. The evolution of K and, more specifically, the characteristic time delay τ_c at which K reaches a plateau (close to the value $K_G = 3$) did not depend on oil viscosity, but τ_c decreased systematically with imposed flow rate. Moreover, the intensity of the intermittent character of the velocity signal measured by the exponent α appeared to be the same for the various experimental conditions. Therefore, rescaling the time lag τ by the characteristic time scale τ_c collapsed the kurtosis for all the experiments, as shown in the inset of the right bottom panel of Fig. 5. We found that $\tau_c \sim 1/\mathrm{v}$ with a proportionality coefficient around 0.6 mm—independently of ℓ, μ, v. This value coincides with ℓ_d, the mean extent of the disorder patches, and thus, $\tau_c = \ell_d/\mathrm{v}$ can be identified as the average time spent by the fluid front to advance over the typical distance ℓ_d. Interestingly, while local bursts of activity can extend on scales much larger than this characteristic length of the medium heterogeneities ℓ_d and last over time scales much longer than τ_c, the latter determines the temporal range of intermittency of the global (spatially averaged) velocity signal.

Finally, this statistical analysis of $\Delta V_\ell(\tau)$ allowed us to reach the main result of our study, namely to identify the controlling parameters of the observed intermittent dynamics. Figure 6 shows the normalized statistical distributions of spatially averaged velocity increments $\Delta V_\ell(\tau)$ obtained under various experimental conditions (μ, v), but measured at length scales ℓ and time lags τ such that both ratios ℓ/ℓ_c and τ/τ_c are fixed. The data collapse shows that the distributions of velocity increments depend specifically on those two parameters only. While the characteristic time τ_c sets the temporal range over which intermittency is observed, the ratio ℓ/ℓ_c controls its intensity.

To conclude, slow imbibition of a disordered confined medium (a laboratory model of an open fracture) showed all the characteristic features of intermittent dynamics. As shown in Fig. 1, periods of low velocities (slightly below the imposed mean front velocity v) alternated with periods of very large velocity excursions above v. In the former, the acceleration was small and strongly correlated to the velocity, while in the latter the acceleration fluctuated strongly. Such intermittent dynamics results from local bursts of fast cooperative motion, triggered from the smallest length scales of the medium heterogeneities up to the correlation length ℓ_c—the scale at which viscous pressure damping becomes more effective than surface tension, which depends upon capillary number and medium permeability. Both ℓ_c and τ_c vanish at high flow rates. Hence, intermittency is present only in slow imbibition displacements in the capillary regime.

By analogy with intermittency and the flux of energy across different scales in fully developed turbulence [13,20], we suggest that the positive asymmetry of the statistical distributions of velocity increments observed in our experiments could be the signature of an inverse cascade resulting from fluid incompressibility, which is at the origin of the correlation length ℓ_c [10]. Extension of the analysis presented here to other problems of front propagation in random media such as fluid imbibition in compact porous media [31], contact line dynamics [32], and planar crack front displacements [33], could bring further insight into this question. Our model experiment of fluid front invasion at low Ca, and the systems mentioned, are very different from hydrodynamic or wave turbulence. Hence, we expect that the results presented in this Letter will motivate new theoretical and experimental approaches of intermittency.

We are grateful to Ramon Planet, Laurent Chevillard, Bernard Castaing, and Sergio Ciliberto for interesting discussions. X. C. acknowledges the financial support of ENS-Lyon through the "Enveloppe attractivité" program and the region Rhône-Alpes, and of MINECO (Spain) through FPU Fellowship No. AP2009-0839. This research received the financial support of MINECO, Spain, Projects No. FIS2010-21924-C02-032 and FIS2013-41144-P, and Generalitat de Catalunya, Projects No. 2009-SGR-14 and No. 2014-SGR-878.

[1] M. Dubé, M. Rost, K. R. Elder, M. Alava, S. Majaniemi, and T. Ala-Nissila, Phys. Rev. Lett. **83**, 1628 (1999).
[2] D. Geromichalos, F. Mugele, and S. Herminghaus, Phys. Rev. Lett. **89**, 104503 (2002).
[3] E. Pauné and J. Casademunt, Phys. Rev. Lett. **90**, 144504 (2003).
[4] J. Soriano, J. Ortín, and A. Hernández-Machado, Phys. Rev. E **66**, 031603 (2002).
[5] M. Rost, L. Laurson, M. Dubé, and M. Alava, Phys. Rev. Lett. **98**, 054502 (2007).
[6] R. Planet, S. Santucci, and J. Ortín, Phys. Rev. Lett. **102**, 094502 (2009); **105**, 029402 (2010).
[7] R. Planet, S. Santucci, and J. Ortín, J. Contam. Hydrol. **120–121**, 157 (2011).
[8] S. Santucci, R. Planet, K. J. Måløy, and J. Ortín, Europhys. Lett. **94**, 46005 (2011).
[9] B. Berkowitz, A. Cortis, M. Dentz, and H. Scher, Rev. Geophys. **44**, RG2003 (2006).
[10] M. Alava, M. Dubé, and M. Rost, Adv. Phys. **53**, 83 (2004).
[11] M. Sahimi, *Flow and Transport in Porous Media and Fractured Rock*, 2nd ed (VCH, New York, 2011).
[12] P. de Anna, T. Le Borgne, M. Dentz, A. M. Tartakovsky, D. Bolster, and P. Davy, Phys. Rev. Lett. **110**, 184502 (2013).
[13] U. Frisch, *Turbulence* (Cambridge University Press, Cambridge, England, 1995).
[14] B. Castaing, Y. Gagne, and E. J. Hopfinger, Physica (Amsterdam) **46D**, 177 (1990).
[15] L. Chevillard, B. Castaing, E. Lévêque, and A. Arneodo, Physica (Amsterdam) **218D**, 77 (2006).
[16] E. Falcon, S. Fauve, and C. Laroche, Phys. Rev. Lett. **98**, 154501 (2007).
[17] E. Falcon, S. G. Roux, and C. Laroche, Europhys. Lett. **90**, 34005 (2010).
[18] G. Falkovitch, K. Gawedzki, and M. Vergassola, Rev. Mod. Phys. **73**, 913 (2001).
[19] A. Arneodo *et al.* (International Collaboration for Turbulence Research), Phys. Rev. Lett. **100**, 254504 (2008).
[20] L. Chevillard, B. Castaing, A. Arneodo, E. Lévêque, J.-F. Pinton, and S. G. Roux, C.R. Phys. **13**, 899 (2012).
[21] The effective permeability of a disordered medium relates the apparent average velocity $\vec{v}$, calculated on the basis of the total flow rate per unit area of the sample cross section, to the applied pressure gradient $\vec{\nabla}P$, in the form $\vec{v} = -(\kappa/\mu)\vec{\nabla}P$, where μ is the dynamic viscosity of the fluid.
[22] K. J. Måløy, S. Santucci, J. Schmittbuhl, and R. Toussaint, Phys. Rev. Lett. **96**, 045501 (2006).
[23] See Supplemental Material at http://link.aps.org/supplemental/10.1103/PhysRevLett.113.074501 for video recordings of the invading front.
[24] A. Dougherty and N. Carle, Phys. Rev. E **58**, 2889 (1998).
[25] V. Privman, in *Finite-Size Scaling and Numerical Simulation of Statistical Systems* (World Scientific, Singapore, 1990).
[26] N. Mallick, P.-P. Cortet, S. Santucci, S. G. Roux, and L. Vanel, Phys. Rev. Lett. **98**, 255502 (2007).
[27] E. Falcon, S. G. Roux, and B. Audit, Europhys. Lett. **90**, 50007 (2010).
[28] S. Santucci, K. J. Måløy, A. Delaplace, J. Mathiesen, A. Hansen, J. Ø. H. Bakke, J. Schmittbuhl, L. Vanel, and P. Ray, Phys. Rev. E **75**, 016104 (2007).
[29] X. Clotet, S. Santucci, and J. Ortín, in *Proceedings of the March CO Meeting'12 "Complex Matter Physics: materials, dynamics and patterns"* (Havana, Cuba, 2012); Rev. Cubana Fís. **29**, 1E62 (2012).
[30] $Sk \equiv E(x - \langle x \rangle)^3/\sigma^3$ and $K \equiv E(x - \langle x \rangle)^4/\sigma^4$, where $E(x - \langle x \rangle)^n$ is the nth central moment of the distribution of x and σ its standard deviation.
[31] T. Delker, D. B. Pengra, and P.-z. Wong, Phys. Rev. Lett. **76**, 2902 (1996).
[32] P. Le Doussal, K. J. Wiese, S. Moulinet, and E. Rolley, Europhys. Lett. **87**, 56001 (2009).
[33] K. T. Tallakstad, R. Toussaint, S. Santucci, and K. J. Måløy, Phys. Rev. Lett. **110**, 145501 (2013).